Multiple-Porosity Contaminant Transport by Finite-Element Method

Abbas H. El-Zein[1]; John P. Carter[2]; and David W. Airey[3]

Abstract: An exponential finite-element model for multiple-porosity contaminant transport in soils is proposed. The model combines three compartments for dissolved contaminants: a primary compartment of diffusion–advection transport with nonequilibrium sorption, a secondary compartment with diffusion in rectangular or spherical soil blocks, and a tertiary compartment for immobile solutions within the primary compartment. Hence the finite-element model can be used to solve four types of mass-transfer problems which include: (1) intact soils, (2) intact soils with multiple sources of nonequilibrium partitioning, (3) soils with a network of regularly spaced fissures, and (4) structured soils. Hitherto, mobile/immobile compartments, fissured soils, and nonequilibrium sorption have been treated separately or in pairs. A Laplace transform is applied to the governing equations to remove the time derivative. A Galerkin residual statement is written and a finite-element method is developed. Both polynomial and exponential finite elements are implemented. The solution is inverted to the time domain numerically. The method is validated by comparison to analytical and boundary element predictions. Exponential elements perform particularly well, speeding up convergence significantly. The scope of the method is illustrated by analyzing contamination from a set of four waste repositories buried in fissured clay.

DOI: 10.1061/(ASCE)1532-3641(2005)5:1(24)

CE Database subject headings: Contaminants; Porosity; Finite element method; Laplace transform; Transport phenomena.

Introduction

Dual-porosity models of contaminant transport in soil have been developed as a way of extending the bicontinuum approach to account for the effect of stagnant liquids undergoing nonequilibrium exchange with a mobile solution (Coats and Smith 1964; van Genuchten 1985; Goltz and Roberts 1986; Brusseau 1991; Hatfield et al. 1993). Such exchange may be due to the presence in the soil of dense nonaqueous liquids or water in dead-end pores. It may also occur in the macropores between the soil aggregates of agricultural top soils, usually referred to as structured soils. A dual-porosity conceptualization has also been used to model contaminant fate in cohesive fissured soils, where transport in the intact matrix blocks is exclusively diffusive (Bibby 1981; Rowe and Booker 1990; Leo and Booker 1996; Elzein 2003a). The soil is idealized as a set of equally spaced fissures separated by intact soil blocks. Other approaches to the modeling of fissured or fractured soils, such as the discrete-fracture approach (Sudicky and McLaren 1992; Therrien and Sudicky 1996), have been used. (The difference between fractured and fissured soils is one of spatial frequency of defects. Fractured soils contain a small number of fractures while fissured soils have a high density of fissures. However, there is no difference in the mathematical formalisms used to represent the two cases.) The dual-porosity concept offers a significant advantage over the discrete-fracture approach in that it does not require a detailed description of fissuring. The concept has been developed further with multiple-porosity formulations incorporating both fissuring and nonequilibrium exchange. The equations have been solved by finite-layer and boundary-element techniques (Elzein 2003a,c). No finite-element models of multiple-porosity mass transfer have yet been developed.

It has long been established that finite-element solutions of the diffusion–advection equations suffer from numerical dispersion problems whenever a significant advection component is present (Daus et al. 1985). For example, the Galerkin time-marching finite-element method (FEM) starts exhibiting significant oscillations around the exact solution at element Péclet numbers greater than 2 (Sudicky 1989). Various ways of improving the performance of numerical solutions have been proposed. Stabilization methods add a term to the residual statement in order to dampen solution oscillations (Brooks and Hughes 1982; Franca and Carmo 1989; Zienkiewicz and Taylor 1991; Franca et al. 1992). The method of second moments, a quasi-Lagrangian technique which offers subgrid scale accuracy, can solve problems with high Péclet numbers (Lupini and Tirabassi 1983). Adaptive discretization schemes have been applied to standard Galerkin formulations as well as stabilized residual statements (Strouboulis and Oden 1990; Agarwal and Pinsky 1996). Such schemes do not reduce numerical dispersion but they allow faster development of an optimal mesh by estimating the solution error. Another approach consists of Laplace transforming the diffusion–advection equations and solving them by conventional finite-element (Brooks and Hughes 1982; Wang and Booker 1997) or boundary-element methods (Leo and Booker 1993; Elzein and Booker 1999a). Pro-

[1]Dept. of Civil Engineering, Centre for Geotechnical Research, Univ. of Sydney, NSW 2006, Australia (corresponding author). E-mail: aelzein@civil.usyd.edu

[2]Dept. of Civil Engineering, Centre for Geotechnical Research, Univ. of Sydney, NSW 2006, Australia.

[3]Dept. of Civil Engineering, Centre for Geotechnical Research, Univ. of Sydney, NSW 2006, Australia.

Note. Discussion open until August 1, 2005. Separate discussions must be submitted for individual papers. To extend the closing date by one month, a written request must be filed with the ASCE Managing Editor. The manuscript for this paper was submitted for review and possible publication on March 24, 2003; approved on January 7, 2004. This paper is part of the ***International Journal of Geomechanics***, Vol. 5, No. 1, March 1, 2005. ©ASCE, ISSN 1532-3641/2005/1-24–34/$25.00.

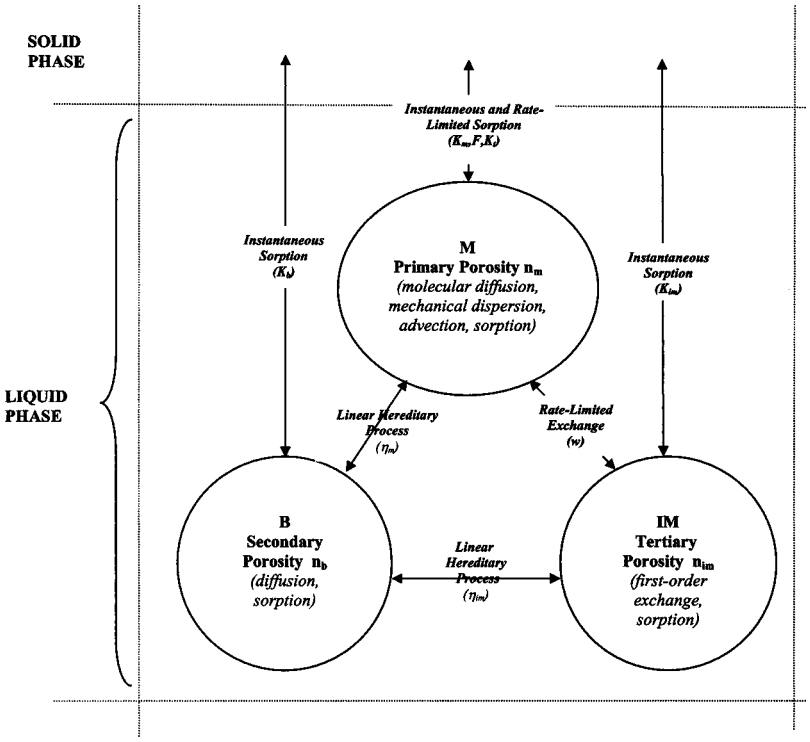

Fig. 1. *POROS* conceptual representation

vided an accurate Laplace-inversion technique is used, numerical dispersion errors of Laplace-domain solutions have been found to be milder than those based on time marching. More recently, an exponential FEM in the Laplace domain, based on nonisoparametric, exponentially varying elements, rather than conventional polynomial elements, has been shown to reduce by about 75% the number of degrees of freedom required for convergence, in the case of single-porosity diffusion–advection problems (Elzein 2003b).

This paper proposes a new exponential FEM for multiple-porosity transport of contaminants in saturated media. A formulation developed earlier by the authors (Elzein 2003c, Elzein and Carter 2003) is extended to include structured soils and the exponential FEM is used to solve the equations. The proposed method is therefore wider in scope than existing mass-transfer formulations for saturated media and can be a better starting point for developing general-purpose diffusion–advection software. It allows, for example, the modeling of structured or fissured soils which contain immobile solutions in the macropores or the fissures, respectively. In addition, the developed algorithm is used to assess whether the accuracy gains from exponential elements extend to the case of contaminant migration with sorption, fissuring, and nonequilibrium exchange.

Multiple-Porosity Model

The proposed model, *POROS*, combines three compartments for dissolved contaminants (Fig. 1): a primary compartment for diffusion–advection transport with nonequilibrium sorption; a secondary compartment with diffusion and linear sorption in rectangular or spherical soil blocks; and a tertiary compartment of immobile solutions within the primary compartment (Elzein 2003c). The latter simulates those reactive processes which can be represented by a first-order rate-limited exchange with the primary compartment.

In other words, a compartment is a medium where dissolved contaminants undergo the same migration and partitioning processes. Example of compartments are fissures, macropores, and immobile solutions. The relative size of each compartment is represented by a porosity.

Exchange between the diffusion-only secondary compartment, on the one hand, and the primary and tertiary compartments, on the other hand, is assumed to follow a linear hereditary process. Exchange between the primary and tertiary compartments is represented by a first-order rate-limited equation. Hence, the model can be used to solve four types of mass-transfer problems and their combinations:

1. intact soils (primary compartment only; single porosity);
2. intact soils with multiple sources of nonequilibrium partitioning (MNEP) (primary compartment for mobile solutions and tertiary compartment for immobile solutions; dual porosity);
3. soils with a 1D, 2D, or 3D network of regularly spaced fissures (primary compartment for mobile solutions in the fissures, secondary compartment for transport in the soil–matrix blocks, and possibly tertiary compartments for immobile solutions in the fissures; dual or multiple porosity); and
4. structured soils with spherical soil–matrix blocks (primary compartment for mobile solutions in the macropores, secondary compartment for transport in the soil matrix blocks, and possibly tertiary compartments for immobile solutions in the macropores; dual or multiple porosity).

Sorption in the primary compartment can be time dependent or instantaneous. Sorption in the secondary and tertiary compartments, on the other hand, is assumed to be instantaneous since the time scale of nonequilibrium sorption is likely to be negligible in

comparison with the long time scale of diffusive-only transport and first-order, rate-limited exchange.

Three mass-conservation statements for the dissolved contaminants can be written as follows:

$$\nabla[\mathbf{v}_a c_m - \nabla(\mathbf{D}_\mathbf{a} c_m)] + n_m \mathbf{R}_m^i \frac{\partial c_m}{\partial t} + \frac{\partial q_m^{\mathrm{ne}}}{\partial t} + n_m \lambda_m c_m + n_{\mathrm{im}} \frac{\partial c_{\mathrm{im}}}{\partial t} + f_m^b = 0 \quad (1)$$

$$n_{\mathrm{im}} R_{\mathrm{im}}^i \frac{\partial c_{\mathrm{im}}}{\partial t} + n_{\mathrm{im}} \lambda_{\mathrm{im}} c_{\mathrm{im}} + f_{\mathrm{im}}^b = w(c_m - c_{\mathrm{im}}) \quad (2)$$

$$\frac{\partial q_m^{\mathrm{ne}}}{\partial t} = k_t\{(1-F) q_m^e - q_m^{\mathrm{ne}}\} \quad (3)$$

where t=time; x_j[L] (j=1,3)=coordinate system; subscripts m and im refer to primary (mobile solution) and tertiary (immobile solution) compartments; respectively; $c_m(t,x_j)$ and $c_{\mathrm{im}}(t,x_j)$ [M L^{-3}]=contaminant concentrations; $\mathbf{v}_a$ [L T^{-1}]=vector of Darcy velocity in the primary compartment resulting from the three components V_1, V_2, and V_3 [L T^{-1}] of seepage velocity in the three directions; $\mathbf{D}_a$ [L^2 T^{-1}]="effective" tensor of hydrodynamic dispersion in the primary compartment; D_{a1}, D_{a2}, and D_{a3}=diagonal components of $\mathbf{D}_\mathbf{a}$ (D_{a12}, D_{a13}, and D_{a23} are assumed to be nil); D_0 [L^2 T^{-1}]=coefficient of diffusion of the contaminant in water at infinite dilution; α_L [L]=dispersivity in the primary compartment, assumed to be the same in all directions; n_m and n_{im}=porosities; λ_m and λ_{im} [T^{-1}]=decay coefficients; $q_m^{\mathrm{ne}}(t,x_j)$ [M M^{-1}]=concentration of contaminant sorbed under nonequilibrium conditions; $q_m^e(x_j)$ [M M^{-1}]=concentration of sorbed contaminant at equilibrium; F=proportion of instantaneous sorption in the primary compartment; R_m^i and R_{im}^i=instantaneous linear sorption retardation factors; R_m and R_{im}=total linear sorption retardation factors; w [T^{-1}]=first-order mass transfer coefficient between the primary and tertiary compartments; k_t [T^{-1}]=first-order sorption rate constant in the primary compartment; f_m^b [M L^{-3} T^{-1}]=rate of exchange between the primary and secondary compartments; and f_{im}^b [M L^{-3} T^{-1}]=rate of exchange between the tertiary and secondary compartments.

It can be easily shown that $R_m^i=(1-F)+FR_m$ and $R_{\mathrm{im}}^i=R_{\mathrm{im}}$. In the case of fissured soils, a treatment of f_m^b and f_{im}^b, proposed by Rowe and Booker (1990), is adopted here. The soil is assumed to be made of n_f (=1, 2, or3) orthogonal fissure planes inbetween rectangular soil–matrix blocks of dimensions H_1, H_2, and H_3 in the three directions, respectively [Fig. 2(a)]. The sizes of the fissure openings are h_1, h_2, and h_3 in the three directions. The method uses the Boltzmann superposition principle and continuity conditions at the interface between a fissure and the adjacent soil–matrix blocks. An analytical expression in the Laplace domain of the rate of exchange between the fissures and the soil blocks is developed.

In the case of structured soils, Huyakorn et al. (1983) presented a formulation for transport in macropores between perfectly spherical lenses of radius r_0 [Fig. 2(b)]. Their solution is adopted here. A solution for the rectangular slabs of fissured soils was also developed in the same paper. However, the formulation later proposed by Rowe and Booker (1990) and used here is more general in scope.

Table 1 shows various combinations of primary, secondary, and tertiary contaminant compartments simulating a number of problems belonging to one of the types defined above. Table 2 shows the range and values of some key parameters for the four problem types. In Table 2, n=porosity in the case of intact soils; n_M=porosity of macropores in the case of structured soils; and D_b, n_b, and R_b=diffusion coefficient, porosity, and retardation factor, respectively, of the rectangular or spherical soil–matrix blocks.

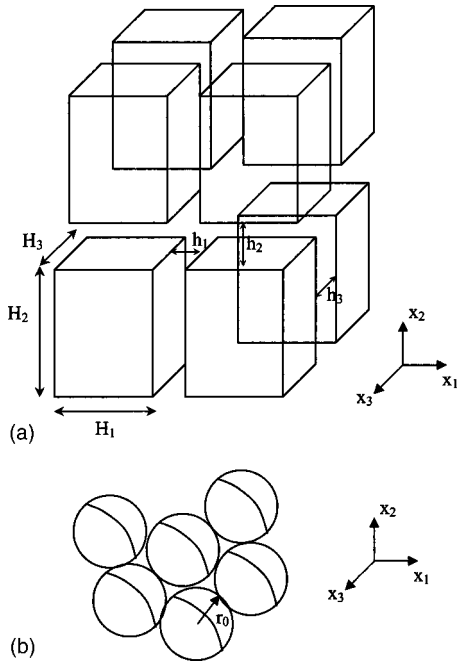

Fig. 2. Soil–matrix blocks as secondary compartments of fissured or structured soils: (a) rectangular soil–matrix blocks for fissured soils (fissure openings are exaggerated for clarity) and (b) spherical soil–matrix blocks for structured soils

Eqs. (1)–(3) can be linearized with respect to time by applying the Laplace transform. A standard finite-element technique can then be applied without resort to time stepping. The main drawback of such an approach is that it cannot deal with temporal variability of input parameters, such as nonsteady-state seepage velocities. However, this limitation is less significant than may at first appear since, in many cases, the lack of detailed geotechnical data does not permit the accurate simulation of such variability anyway and assumptions of steady-state flow are routinely made in simulations.

The Laplace transform can be defined as follows:

$$\overline{g}(s) = \int_0^\infty e^{-\mathrm{st}} g(t)\,dt \quad (4)$$

Applying the Laplace transform to Eqs. (1)–(3) and incorporating the kinetics of exchange between the three compartments, the following equations can be written (Elzein 2003c):

$$\mathbf{D}_\mathbf{a}\nabla^2\overline{c_m} - \mathbf{v}_\mathbf{a}\nabla\overline{c_m} = \overline{\Phi}_m\overline{c_m} - \overline{\Phi}_{m0}c_{m0} \quad (5)$$

$$\overline{c_{\mathrm{im}}} = \overline{A}_{\mathrm{im}}\overline{c_m} + \overline{B}_{\mathrm{im}}c_{\mathrm{im0}} \quad (6)$$

$$\overline{q_m^{\mathrm{ne}}} = \overline{A}_{\mathrm{ne}}\overline{c_m} + \overline{B}_{\mathrm{ne}}q_{m0}^{\mathrm{ne}} \quad (7)$$

$$\overline{q_m^e} = n_m(R_m - 1)\overline{c_m} \quad (8)$$

Table 1. Problem Types and Compartment Definitions

Problem type		Problem description	Primary compartment	Secondary compartment	Tertiary compartment	Parameters
Type I: intact soils	A	With linear sorption	Pores of intact soil	Nonexistent	Nonexistent	$n_{im}=0$ $F=1$ $h_1=h_2=h_3=0$ $r_0=0$
Type II: intact soils with nonequilibrium processes	B	With nonequilibrium sorption	Pores of intact soil	Nonexistent	Nonexistent	$n_{im}=0$ $h_1=h_2=h_3=0$ $r_0=0$
	C	With multiple nonequilibrium processes	Pores of intact soil	Nonexistent	Immobile solution in pores of intact soil	$h_1=h_2=h_3=0$ $r_0=0$
Type III: fissured soil	E	Fissure network	Fissures	Soil–matrix blocks with diffusion and linear sorption	Nonexistent	$n_{im}=0$ $F=1$ $r_0=0$
	F	Fissure network	Fissures	Nonexistent	Soil–matrix pores	$F=1$ $h_1=h_2=h_3=0$ $r_0=0$
	G	Fissure network with multiple nonequilibrium processes	Fissures	Soil–matrix blocks with diffusion and linear sorption	Immobile solution in fractures	$r_0=0$
Type IV: structured soils	H	Structured soil	Macropores	Soil–matrix spherical pores	Nonexistent	$n_{im}=0$ $F=1$ $h_1=h_2=h_3=0$
	I	Structured soil	Macropores	Nonexistent	Soil–matrix pores	$F=1$ $h_1=h_2=h_3=0$ $r_0=0$
	J	Structured soil with multiple nonequilibrium processes	Macropores	Soil–matrix spherical pores	Immobile solution in macropores	$h_1=h_2=h_3=0$

$$\overline{q}^{e}_{im} = n_{im}(R_{im}-1)\overline{c}_m \tag{9}$$

where

$$\overline{\Phi}_m = (n_m\overline{r}_m + n_{im}\overline{A}_{im} + \overline{A}_{ne})s + n_m\lambda_m + \overline{\eta}_m\lambda_b \tag{10}$$

$$\overline{\Phi}_{m0} = n_m\overline{r}_m + n_{im}(1 - s\overline{B}_{im}) + n_m(1-F)(R_m-1)(1-s\overline{B}_{ne}) \tag{11}$$

$$\overline{A}_{im} = \frac{w}{n_{im}\overline{r}_{im}s + w + n_{im}\lambda_{im} + \lambda_b\overline{\eta}_{im}} \tag{12}$$

$$\overline{B}_{im} = \frac{n_{im}\overline{r}_{im}}{w}\overline{A}_{im} \tag{13}$$

$$\overline{A}_{ne} = \frac{n_m k_t(1-F)(R_m-1)}{s+k_t} \tag{14}$$

$$\overline{B}_{ne} = \frac{1}{s+k_t} \tag{15}$$

$$\overline{r}_m = R^i_m + \frac{\overline{\eta}_m}{n_m} \tag{16}$$

$$\overline{r}_{im} = R^i_{im} + \frac{\overline{\eta}_{im}}{n_{im}} \tag{17}$$

where $c_{m0}(t,x_j)=c_m(0,x_j)$; $c_{im0}(t,x_j)=c_{im}(0,x_j)$; $q^e_{im}(x_j)$ = concentration of sorbed contaminant at equilibrium in the ter-

Table 2. Key Parameters for Four Problem Types

	Type I: intact soils (single porosity)	Type II: intact soils with nonequilibrium exchange (dual porosity)	Type III: fissured soils (triple porosity)	Type IV: structured soils (triple porosity)
n_m	n	0–1	$h_1/H_1+h_2/H_2+h_3/H_3$	n_M
D_{ai}	$n(D_0+\alpha_L V_i)$	$n(D_0+\alpha_L V_i)$	$\gamma_i(D_0+\alpha_L V_i)$	$n_M(D_0+\alpha_L V_i)$
V_{ai}	nV_i	nV_i	$\gamma_i V_i$	$n_M V_i$
γ_i	NA[a]	NA[a]	$h_1(1-\delta_{i1})/H_1+h_2(1-\delta_{i2})/H_2$ $+h_3(1-\delta_{i3})/H_3$	NA[a]

Note: δ_{pq}=Dirac delta function ($\delta_{pq}=1$ when $p=q$ and $\delta_{pq}=0$ when $p\neq q$).

[a]NA=not applicable.

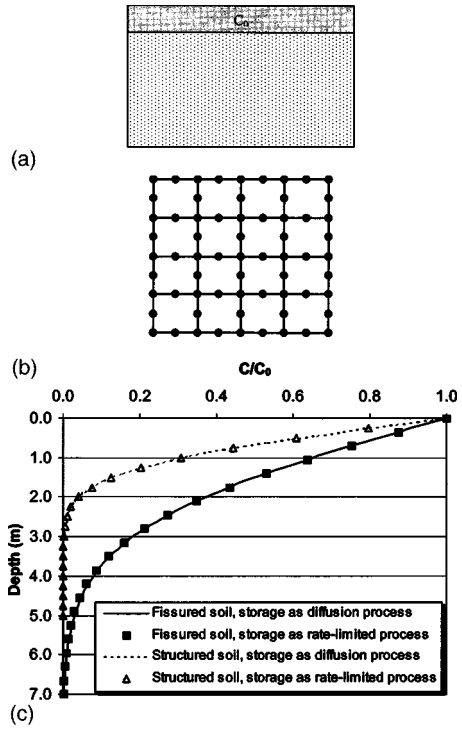

Fig. 3. Problems 1 and 2: comparison of dual-porosity predictions from first-order, rate limited model and diffusion-only model: (a) geometry; (b) converged finite-element mesh: 16 E8 elements; and (c) contamination profiles along depth: $t=500$ years for fissured clay of problem 1 and $t=2$ weeks for structured sand of problem 2

tiary compartment; $\eta_m(t)$=coefficient of exchange between the primary and secondary compartments; and $\eta_{\text{im}}(t)$=coefficient of exchange between the tertiary and secondary compartments. Expressions for $\overline{\eta_m}$ and $\overline{\eta_{\text{im}}}$ are given analytically in Appendices I and II for fissured and structured soils.

A number of experimental methods have been developed to measure diffusion coefficients, sorption in the soil matrix blocks, seepage velocity, porosity, soil density, and fracture openings. These methods are well documented in the literature. However, other parameters in the model present more difficulties. The extent of immobile solutions in the soil pores is usually difficult to establish. Nevertheless, methods for estimating the exchange rate w and the immobile porosity n_{im} have been suggested (Brusseau et al. 1989). On the other hand, very little research has been conducted on sorption against fissure walls and no experimental methods for quantifying the process have been developed. The inverse solution of the proposed model is one possible way of determining fissure sorption coefficients, pending the development of robust experimental procedures.

Exponential Finite Elements

A Galerkin finite-element statement of the two-dimensional version of Eq. (5) can be written as follows:

$$\int_{\Omega} N_i(x_1,x_2)\{\mathbf{D_a}\nabla^2\overline{c_m} - \mathbf{v_a}\nabla\overline{c_m} - \overline{\Phi}_m\overline{c_m}\}d\Omega = 0 \qquad (18)$$

where Ω=domain of the problem and $N_i(x_1,x_2)$=interpolation functions of the elements, used as weighing functions of the re-

Table 3. Material Properties for Problems 1–5

Parameters	Units	Problem 1 (leaching into a fissured clay)	Problem 2 (leaching into a structured sand)	Problem 3 (single repository in a fissured clay)	Problem 4 (storage tank in a sand)	Problem 5 (four repositories in a fissured clay)
H_1,H_2,H_3	m	∝,0.01,∝	NA[a]	0.001,0.001,∝	NA[a]	0.1,0.1,∝
h_1,h_2,h_3	m	0,1E−4,0	0,0,0	1E−4,1E−4,0	0,0,0	1E−3,1E−3,0
r_0	m	0	0.1	0	0	0
N	ND[b]	NA[a]	NA[a]	NA[a]	0.28	NA[a]
n_M	ND[b]	NA[a]	0.5	NA[a]	NA[a]	NA[a]
D_0	$m^2\,s^{-1}$	3.17E−10	6.34E−8	3.17E−10	3.17E−8	3.17E−10
α_L	m	1.0	0	5	0.1	5
V_x	$m\,s^{-1}$	3.17E−10	6.34E−8	3.17E−10	3.17E−7	3.17E−10
V_y	$m\,s^{-1}$	0	0	0	0	0
n_m	ND[b]	0.01	0.5	0.2	0.28	0.02
n_{im}	ND[b]	0	0	0.1	0.07	0
R_m	ND[b]	1.0	1.0	11	1.25	1.0
R_{im}	ND[b]	1.0	1.0	21	11	1.0
W	s^{-1}	NA[a]	NA[a]	NA[a]	3.17E−10	NA[a]
k_t	s^{-1}	NA[a]	NA[a]	NA[a]	3.17E−10	NA[a]
F	ND[b]	1.0	1.0	1.0	0.7	NA[a]
n_b	ND[b]	0.1	0.3	0.35	NA[a]	0.35
D_b	$m^2\,s^{-1}$	3.17E−14	3.17E−8	3.17E−14	NA[a]	3.17E−12
R_b	ND[b]	1.0	1.0	1.0	NA[a]	1.0
λ_b	s^{-1}	0	0	3.17E−11	NA[a]	0
λ_m and λ_{im}	s^{-1}	0	0	3.17E−11	3.17E−11	0

Note: Variables in italics are calculated from other parameters according to Table 2.

[a]NA=not applicable.

[b]ND=dimensionless.

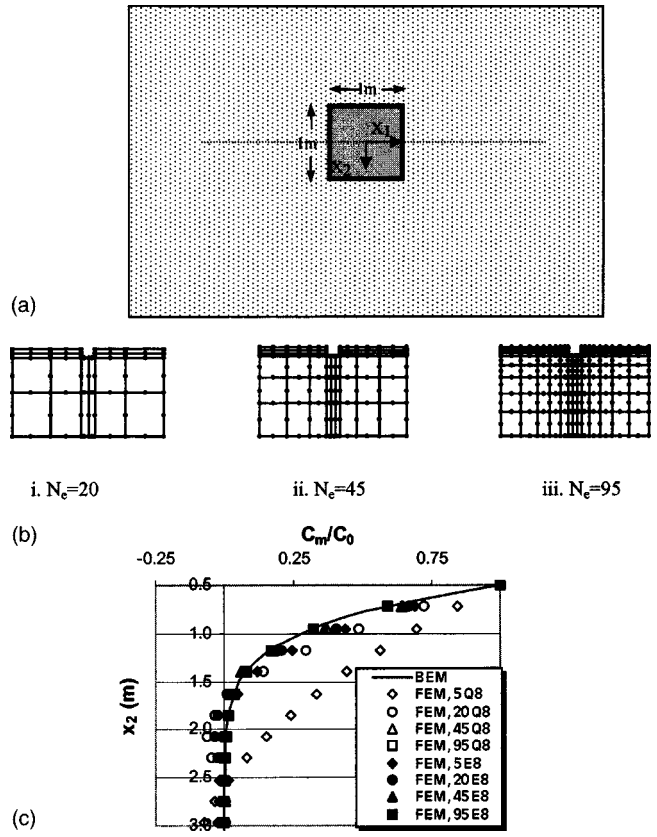

Fig. 4. Problem 3: performance of exponential elements in case of fissured soils: (a) geometry: waste repository in fissured clay (not to scale); (b) finite-element meshes (not to scale); and (c) contamination profile at $t=500$ years along depth at $x_1=0$

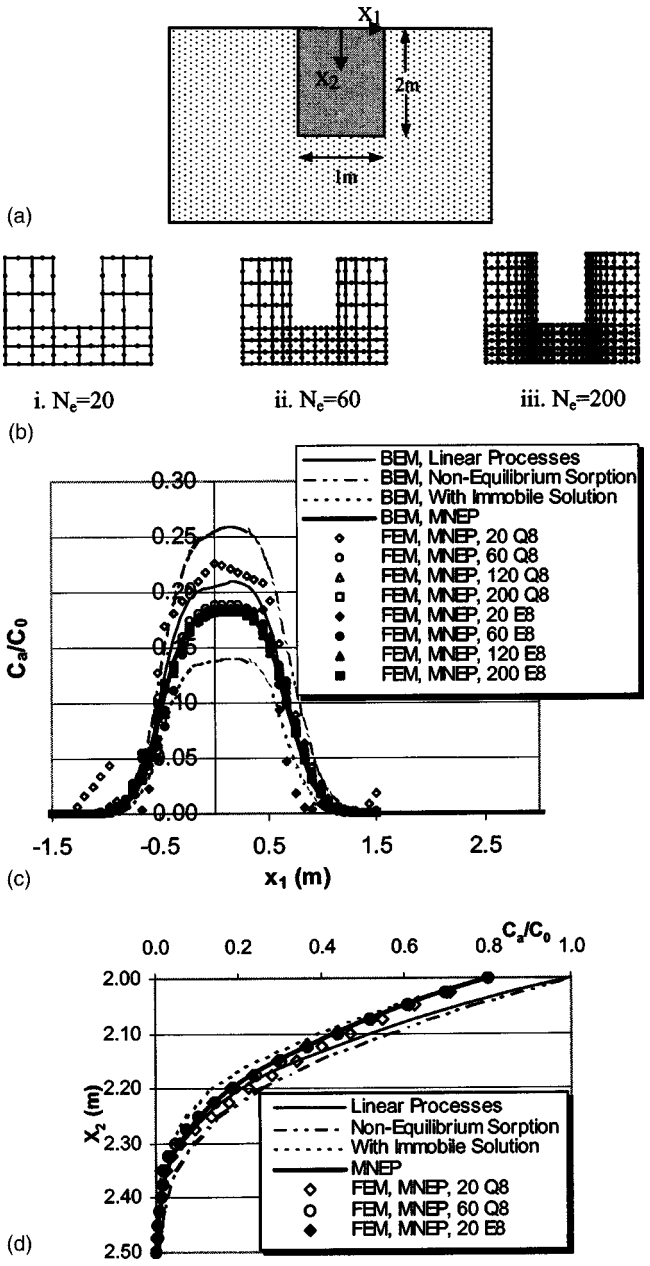

Fig. 5. Problem 4: performance of exponential elements in case of multiple sources of nonequilibrium partitioning: (a) geometry: underground storage tank in sandy soil (not to scale); (b) finite-element meshes (not to scale); (c) contamination profile at $t=2$ weeks, along x_1 axis, at $x_2=2.2$ m; and (d) contamination profile at $t=2$ weeks, along x_2 axis, at $x_1=0$

sidual statement. (c_{m0} has been assumed to be zero in Eq. (18) for the sake of simplicity. However, nonzero c_{m0} can be easily incorporated in the formulation).

Two types of elements can be used to discretize Eq. (18). The first type of elements is the conventional rectangular isoparametric element, based on polynomial shape and interpolation functions. However, it is known that this approximation introduces numerical dispersion into the solution when an advection component is present (Daus et al. 1985; Zienkiewicz and Taylor 1991). Elzein (2003b) proposed nonisoparametric eight-noded elements based on exponential interpolation functions and showed that their performance is superior to that of polynomial elements. Eight-noded exponential elements are implemented here and their performance under conditions of nonequilibrium exchange and/or fissuring is tested. The interpolation functions for an eight-noded exponential element (E8) can be written as follows (Elzein 2003b):

$$N_i(x_1,x_2) = e^{a_i(x_1-x_1^c)+b_i(x_2-x_2^c)} \tag{19}$$

where x_1^c and x_2^c = coordinates of the element's centroid and a_i and b_i are defined as follows:

$$a_i = \{z_{a1}\ z_{a2}\ 0\ 0\ z_{a1}\ z_{a1}\ z_{a2}\ z_{a2}\} \tag{20}$$

$$b_i = \{0\ 0\ z_{b1}\ z_{b2}\ z_{b1}\ z_{b2}\ z_{b1}\ z_{b2}\} \tag{21}$$

$$z_{a1},z_{a2} = \frac{V_1 \pm \sqrt{V_1^2 + 4D_{a1}\Phi_m}}{2D_{a1}} \tag{22}$$

$$z_{b1},z_{b2} = \frac{V_2 \pm \sqrt{V_2^2 + 4D_{a2}\Phi_m}}{2D_{a2}} \tag{23}$$

The interpolation functions of E8, defined by Eqs. (19)–(23), are simple products of the solutions to the one-dimensional form of Eq. (5). The shape functions for E8, on the other hand, are conventional polynomials. Standard eight-noded quadratic elements (Q8) are also implemented (Zienkiewicz and Taylor 1989).

Integrating Eq. (18) by parts and applying the divergence theorem, an algebraic system of equations is obtained with nodal concentrations $\overline{c_m}$ as unknowns. The system is solved and the solution is inverted to the time domain numerically using a scheme devel-

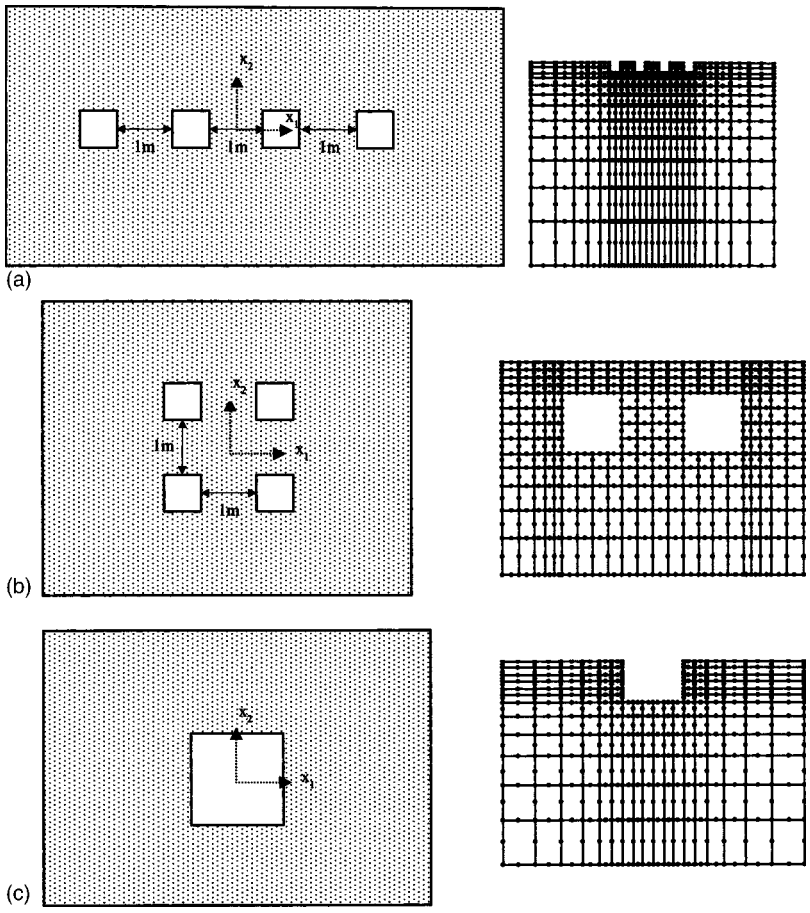

Fig. 6. Problem 5: 4 m^2 underground waste storage in fissured clay soil (symmetry with respect to x_1 axis is used in analyses; figures not to scale): (a) arrangement 1, four 1×1 m^2 repositories arranged in line ($N_e=272$); (b) arrangement 2, four 1×1 m^2 repositories arranged in square ($N_e=254$); and (c) arrangement 3, single 2×2 m^2 repository ($N_e=180$)

oped by Crump (1976). The choice of Laplace-inversion algorithm is made on the basis of computational efficiency. The Crump algorithm offers a significant advantage over other schemes in that the number of s values for which the Laplace-transformed equations must be solved is independent of the number of time stations at which the solution is required.

Results

Validation of Algorithm

Simple one-dimensional problems are first used to validate the method. Various combinations of parameters, replicating the four types of problems shown in Table 1, are tested and results are compared to analytical or finite-layer solutions (Sudicky 1989; Rowe and Booker 1990; Brusseau 1991). Very good agreement between the different approaches is found.

Two additional tests are conducted. Sudicky (1989) has established the equivalence between dual-porosity formulations which incorporate diffusion into matrix blocks explicitly and those which represent storage as an immobile solution governed by a first-order, rate-limited exchange process. He derived the following equivalence relationships:

$$w=\frac{12n_bD_b}{H_1^2} \tag{24}$$

$$w=\frac{15n_bD_b}{r_0^2} \tag{25}$$

Eq. (24) is an expression of the rate of first-order exchange for a soil with a single fissure plane with block size H_1. Eq. (25) is the rate of first-order exchange for a structured soil with spherical lenses of radii r_0.

Since the present formulation incorporates both diffusion into soil blocks and immobile compartments, dual-porosity soils are simulated using both approaches, according to formulas (24) and (25), and results are compared. (The two approaches are reflected in Table 2 by problem types E and F for fissured soils and H and I for structured soils.) The two tests are conducted for semi-infinite soils subject to a uniform source of constant concentration at the surface [Fig. 3(a)]. Data for the problems, designated as Problems 1 and 2, are given in Table 3. Problem 1 is a fissured clay and Problem 2 is a structured sand. A convergence analysis is conducted for each problem to establish the optimal finite-element mesh and the final discretization is shown in Fig. 3(b).

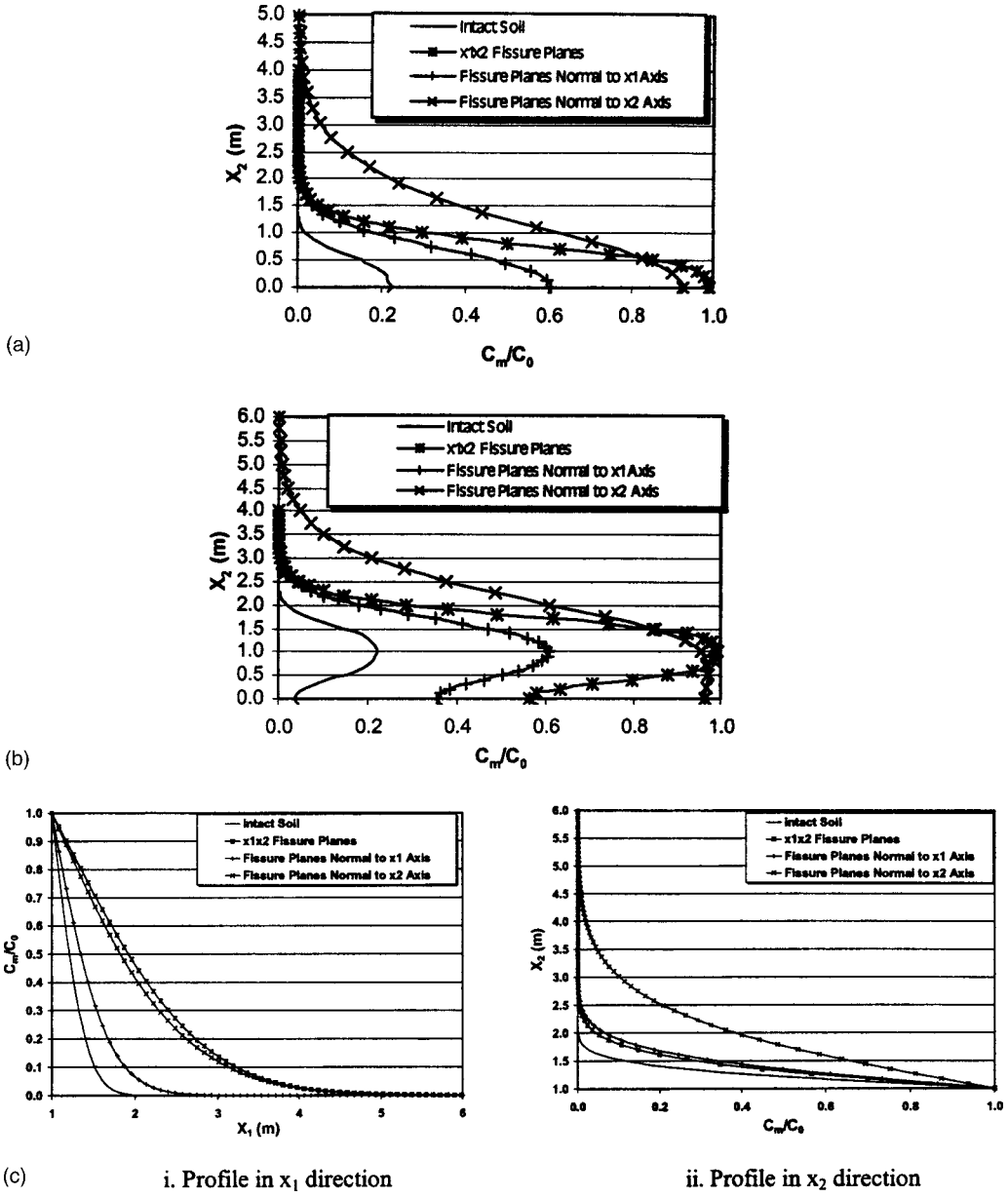

Fig. 7. Problem 5: effects of fissuring patterns on contamination profiles: (a) arrangement 1: profile in x_2 direction; (b) arrangement 2: profile in x_2 direction; and (c) arrangement 3

Concentration profiles along the depth are shown for both problems in Fig. 3(c). There is clearly very good agreement between the two approaches.

Performance of Exponential Elements under Dual-Porosity Conditions

The ability of exponential elements to speed up convergence under dual-porosity conditions is assessed through Problems 3 and 4. Material properties for both problems are shown in Table 3. Symmetry around the x_1 axis is used in the analyses. Finite elements predictions are compared to results from converged boundary element simulations (Elzein and Booker 1999b).

Problem 3 is a square-shaped repository buried in a fissured clay [Fig. 4(a)]. Concentration of contaminant in the repository is assumed to be constant at C_0. As shown in Fig. 4(b), finite-element meshes with increasing number of elements are used. Fig. 4(c) shows the contamination profile along a vertical line below the center of the repository. Exponential elements clearly produce more accurate results than polynomial elements, speeding up convergence significantly.

Problem 4, shown in Fig. 5(a), is an underground storage tank leaking into a sandy soil. Contaminant transport is accompanied by multiple sources of nonequilibrium exchange: 30% of sorption is time dependent and 20% of pores are occupied by an immobile solution. Finite-element meshes shown in Fig. 5(b) are used in the analysis. The weighted-average concentration C_a, taking into account immobile solutions, is defined as

$$C_a = \frac{n_m C_m + n_{\text{im}} C_{\text{im}}}{n_m + n_{\text{im}}} \tag{26}$$

Figs. 5(c and d) show the contamination profiles along the x_1 and x_2 axes, respectively, for the case of simultaneous time-dependent

sorption and exchange with an immobile-phase solution. In addition, results from simulations incorporating single or no sources of nonequilibrium exchange are shown to highlight the effect of time-dependent exchange. Exponential elements converge earlier than polynomial elements once again. However, in Fig. 5(c), close to the two vertical lines of the profile along the x_1 axis, exponential elements sometimes yield less accurate results. Elzein (2003b) showed that exponential elements improve accuracy in 1D and 2D problems. However, it appears that the efficiency of exponential elements is reduced under conditions of strong advection transport.

Illustrative Example

To illustrate the scope of the proposed method, Problem 5 is analyzed next. The problem consists of a set of repositories, carrying a total of 4 m^2 of waste and buried in a clayey soil. Data for the problem are given in Table 3. Three different arrangements of the repositories are suggested in Fig. 6. The purpose of the simulations is to find out which of the three arrangements yields the slowest transport in the x_2 direction and whether fissuring configurations have an effect on the answer. Four fissuring patterns have been simulated: intact soils (no fissures), a set of fissure planes normal to the x_1 axis, a set of fissure planes normal to the x_2 axis, and two sets of fissure planes normal to the x_1 and x_2 axes, respectively. The latter is referred to as "x_1x_2 fissure planes." The concentration of pollutants in the repositories is assumed to remain constant at C_0 throughout the time frame of the analysis. Finite-element meshes used in the analyses are also shown in Fig. 6. All meshes are made of eight-noded exponential elements. All results shown are for $t=500$ years.

Fig. 7 shows the effect of different fissuring patterns on the contamination profiles. Transport in intact soils is clearly slower than all three cases of fissured soils. The existence of fissure planes that are normal to the x_2 axis yields faster transport in the x_2 direction. This may appear counterintuitive. However, since the advection vector is aligned with the x_1 axis, there is advective–diffusive transport in fissure planes normal to the x_2 axis. In the case of fissure planes normal to the x_1 axis, on the other hand, contaminants spread only by diffusion. Hence in both cases, the pollution plume is advancing by diffusion only in the x_2 direction. However, in the case of fissure planes normal to the x_2 axis, the contaminant is spreading in the x_2 direction from a wider x_1 base due to the diffusive–advective transport in the x_1 direction, especially given the relatively large dispersivity factor. Further analyses, not shown here, with smaller dispersivity factors have confirmed this conclusion. In addition, Fig. 7(c.ii) shows that, as expected, contaminants spread faster in the x_1 direction when a fracture plane, normal to the x_2 direction, is present.

Fig. 8 compares the effects of different repository arrangements on the contamination profiles. In all cases of fissuring, arrangement 1 yields the slowest transport of contaminants in the x_2 direction after 500 years. This finding is not surprising since two of the repositories in arrangement 2 are located higher on the x_2 axis than in arrangement 1. In the case of arrangement 3, the line $x_1=0$ at which pollution is depicted is closer to the source of contamination than in arrangement 1. However, when fissure planes are normal to the x_2 axis [Fig. 8(c)], contaminants travel further and the arrangement of repositories has less effect on the speed of transport than in other cases of fissuring.

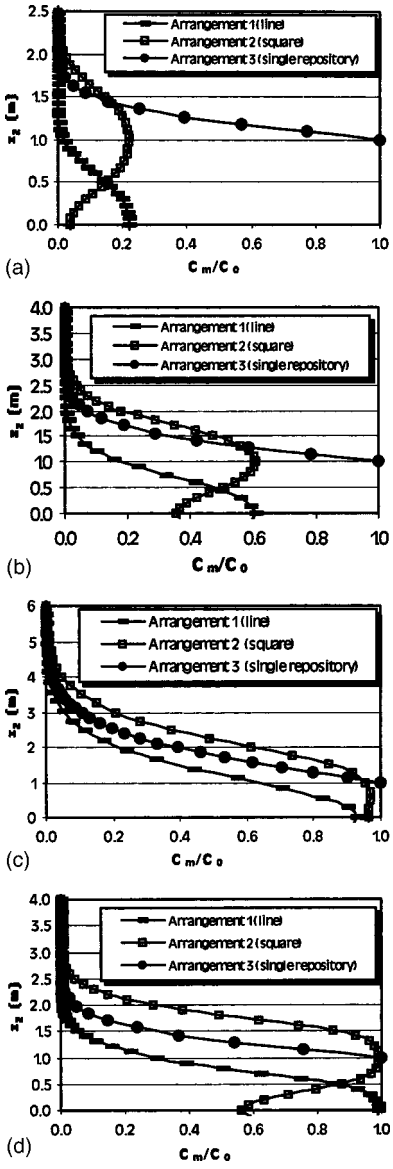

Fig. 8. Problem 5: effects of repository arrangements on contamination profiles: (a) intact soil; (b) fissure planes normal to x_1 axis; (c) fissure planes normal to x_2 axis; and (d) two sets of fissure planes normal to x_1 and x_2 axis, respectively

Conclusions

A new Galerkin finite-element method has been proposed, formulated, and validated. The method can solve, in addition to intact soils, three different types of dual- and multiple-porosity problems, namely soils with nonequilibrium sorption and immobile solutions, fissured clayey soils, and structured topsoils. The algorithm is therefore wider in scope than existing mass-transfer formulations for saturated soils.

Exponential finite elements have been shown to be effective in reducing numerical dispersion errors in the cases of fissured soils and nonequilibrium sorption. The parametric studies performed on the problem of waste repositories buried in soil have shown that the direction of groundwater flow is as important as that of the fissure planes in determining the effect of fissuring on the speed of contamination. In addition, spreading the waste over a number of small repositories along a direction x_i rather than using

a square arrangement or one large repository, can slow down the spread of contamination plumes in directions normal to x_i.

The development of three-dimensional exponential finite-element solutions of multiple-porosity problems is an obvious extension of this work that the authors are pursuing.

Appendix I. Fissured Soils: Rectangular Blocks

Expressions for η have been derived by Rowe and Booker (1990) in the Laplace domain for a set of fissures running between rectangular blocks.

For $n_f=1$

$$\overline{\eta} = n_b R_b \left[1 - 2\sum_{i=1}^{\infty} \left\{ \frac{s+\lambda_b}{s+\lambda_b + \frac{D_b}{R_b}\alpha_i^2} \frac{1}{(\alpha_i H_1)^2} \right\} \right]$$

For $n_f=2$

$$\overline{\eta} = n_b R_b \left[1 - 4\sum_{i,j=1}^{\infty} \left\{ \frac{s+\lambda_b}{s+\lambda_b + \frac{D_b}{R_b}(\alpha_i^2+\beta_j^2)} \frac{1}{(\alpha_i H_1)^2} \frac{1}{(\beta_j H_2)^2} \right\} \right]$$

For $n_f=3$

$$\overline{\eta} = n_b R_b \left[1 - 8\sum_{i,j,k=1}^{\infty} \left\{ \frac{s+\lambda_b}{s+\lambda_b + \frac{D_b}{R_b}(\alpha_i^2+\beta_j^2+\gamma_k^2)} \times \frac{1}{(\alpha_i H_1)^2} \frac{1}{(\beta_j H_2)^2} \frac{1}{(\gamma_k H_3)^2} \right\} \right]$$

$$\alpha_i = \frac{\pi\left(i-\frac{1}{2}\right)}{H_1}$$

$$\beta_j = \frac{\pi\left(j-\frac{1}{2}\right)}{H_2}$$

$$\gamma_k = \frac{\pi\left(k-\frac{1}{2}\right)}{H_3}$$

Appendix II. Structured Soils: Spherical Blocks

Expressions for η have been derived by Huyakorn et al. (1983) in the Laplace domain for a set of macropores surrounded by spherical soil–matrix blocks

$$\overline{\eta} = \frac{3 n_b D_b}{r_0} \left[\chi_b \coth(\chi_b r_0) - \frac{1}{r_0} \right]$$

$$\chi_b = \sqrt{\frac{s R_b}{D_b}}$$

References

Agarwal, A. N., and Pinsky, P. M. (1996). "Stabilized element residual method (SERM): A posteriori error estimation for the advection-diffusion equation." *J. Comput. Appl. Math.*, 74, 3–17.

Bibby, R. (1981). "Mass transport of solutes in dual-porosity media." *Water Resour. Res.*, 17(4), 1075–1081.

Brooks, A. N., and Hughes, T. J. R. (1982). "Streamline upwind/Petrov–Galerkin formulations for convective dominated flows with particular emphasis on the incompressible Navier-Stokes equations." *Comput. Methods Appl. Mech. Eng.*, 32, 199–259.

Brusseau, M. L. (1991). "Application of a multi-process nonequilibrium sorption model to solute transport in a stratified porous medium." *Water Resour. Res.*, 27(4), 589–595.

Brusseau, M. L., Jessup, R. E., and Rao, P. S. C. (1989). "Modeling the transport of solutes influenced by multiprocess non-equilibrium." *Water Resour. Res.*, 25, 1971–1988.

Coats, K. H., and Smith, B. D. (1964). "Dead-end pore volume and dispersion in porous media." *Soc. Pet. Eng. J.*, 4, 73–84.

Crump, K. S. (1976). "Numerical inversion of Laplace transforms using a Fourier series approximation." *J. Assoc. Comput. Math.*, 23(1), 89–96.

Daus, A. D., Frind, E. O., and Sudicky, E. A. (1985). "Comparative error analysis in finite element formulations of the advection-dispersion equation." *Adv. Water Resour.*, 8, 86–95.

Elzein, A. H., and Booker, J. R. (1999a). "Groundwater pollution by organic compounds: A two-dimensional solution of contaminant transport equations in stratified porous media with multiple non-equilibrium partitioning." *Int. J. Numer. Analyt. Meth. Geomech.*, 23, 1717–1732.

Elzein, A. H., and Booker, J. R. (1999b). "Groundwater pollution by organic compounds: A three-dimensional solution of contaminant transport equations in stratified porous media with multiple non-equilibrium partitioning." *Int. J. Numer. Analyt. Meth. Geomech.*, 23, 1733–1762.

Elzein, A. H. (2003a). "Contaminant transport in fissured soils by three-dimensional boundary elements." *Int. J. Geomech.*, 3(1/2), 75–83.

Elzein, A. H. (2003b). "Exponential finite elements for diffusion-advection problems." *Int. J. Numer. Methods Eng.*, in press.

Elzein, A. H. (2003c). "Multiple-porosity model for the transport of reactive contaminants in fractured soils with nonequilibrium partitioning." *Int. J. Geomech.*, 3(3/4), 182–190.

Elzein, A. H., and Carter, J. P. (2003). "A multiple-porosity finite element model for reactive contaminants in soils." *Proc., 2nd MIT Conf. on Computational Fluid and Solid Mechanics*, Cambridge, U.K.

Franca, L. P., and do Carmo, E. G. D. (1989). "The Galerkin gradient least-squares method." *Comput. Methods Appl. Mech. Eng.*, 74, 41–54.

Franca, L. P., Frey, S. L., and Hughes, T. J. R. (1992). "Stabilized finite element methods: I. Application to the advective-diffusive model." *Comput. Methods Appl. Mech. Eng.*, 95, 253–276.

Goltz, M. N., and Roberts, P. V. (1986). "Three-dimensional solutions for solute transport in infinite medium with mobile and immobile zones." *Water Resour. Res.*, 22, 113–1148.

Hatfield, K., Ziegler, J., and Burris, D. R. (1993). "Transport in porous media containing residual hydrocarbon. II: Experiments." *J. Environ. Eng.*, 119(3), 559–575.

Huyakorn, P. S., Lester, B. H., and Mercer, J. W. (1983). "An efficient finite element technique for modelling transport in fractured porous media, 1. Single species transport." *Water Resour. Res.*, 19(3), 841–854.

Leo, C. J., and Booker, J. R. (1993). "Boundary element analysis of contaminant transport in fractured porous media." *Int. J. Numer. Analyt. Meth. Geomech.*, 17, 471–492.

Leo, C. J., and Booker, J. R. (1996). "A time-stepping finite element method for analysis of contaminant transport in fractured porous media." *Int. J. Numer. Analyt. Meth. Geomech.*, 20, 847–864.

Lupini, R., and Tirabassi, T. (1983). "Solution of the advection-diffusion

equation by the moments method." *Atmos. Environ.,* 17(5), 965–971.
Rowe, R. K., and Booker, J. R. (1990). "Contaminant migration in a regular two- or three-dimensional fractured network: reactive contaminants." *Int. J. Numer. Analyt. Meth. Geomech.,* 14, 401–425.
Strouboulis, T., and Oden, J. T. (1990). "A posteriori error estimation of finite element approximations in fluid mechanics." *Comput. Methods Appl. Mech. Eng.,* 78, 201–242.
Sudicky, E. A. (1989). "The Laplace transform Galerkin technique: A time-continuous finite element theory and application to mass transport in groundwater." *Water Resour. Res.,* 25, 1833–1846.
Sudicky, E. A., and McLaren, R. G. (1992). "The Laplace transform Galerkin technique for large-scale simulation of mass transport in discreetly fractured porous formations." *Water Resour. Res.,* 28(2), 499–514.
Therrien, R., and Sudicky, E. A. (1996). "Three-dimensional analysis of variably-saturated flow and solute transport in discreetly-fractured porous media." *J. Contam. Hydrol.,* 23, 1–44.
van Genuchten, M. Th. (1985). "A general approach for modeling solute transport in structured soils." *Proc., Hydrog. Locks Low Hydr. Conduct., Memoirs Int. Assoc. Hydrog.,* 17(1), 513–526.
Wang, J. C., and Booker, J. R. (1997). "A Laplace transform finite element method (LTFEM) for the analysis of contaminant transport in porous media." *Research Rep. No. R756,* Civil Engineering Dept., Univ. of Sydney, Sydney, Australia.
Zienkiewicz, O. C., and Taylor, R. L. (1989). *The finite element method,* 4th Ed., Vol. 1, McGraw-Hill, London, 116.
Zienkiewicz, O. C., and Taylor, R. L. (1991). *The finite element method,* 4th Ed., Vol. 2, McGraw-Hill, London, 461–484.